Effect Of The Fixed Horizontal Tail On Flight Characteristics In Circling

G. Stich
Institut für Flugmechanik
Braunschweig
December, 1982

Translated by Fred Hermanspann

ABSTRACT

Many flight characteristic evaluations of sailplanes with fixed horizontal tails have shown that the flight handling in circling, especially in turbulent thermals, is influenced by the horizontal tail design. Degraded circling flight characteristics reduce the climb performance and affect the cross country speeds, especially in typical European weather conditions.

Starting with the mechanics of circling and the aerodynamics of the horizontal tail, the effects of the following items on circling characteristics are evaluated using the ASW-19 as an example:

1. Location of center of gravity (C.G.)
2. Bank angle in circling
3. Wing lift coefficient increase
4. Wing loading change

Finally, horizontal tail designs are presented that reduce the disadvantages of the fixed horizontal tail regarding circling flight characteristics.

SYMBOLS

A	Lift
AF	Lift of Wing
AH	Lift of Horizontal Tail
b	Wing Span
b_H	Horizontal Tail Span
c_A	Airplane Lift Coefficient
c_a	Sectional Lift Coefficient
c_{AF}	Wing Lift Coefficient
c_{AH}	Horizontal Tail Lift Coefficient
c_{M25}	Zero-lift Moment Coefficient
c_w	Sectional Drop Coefficient
$dc_A/d\alpha$	Wing Lift Slope
$dc_{AH}/d\alpha$	Horizontal Tail Lift Slope
G kg	Weight
$g = 9.80665\ m/s^2$	Gravitational Constant
l_μ	Mean Aerodynamic Chord (M.A.C.)
$N25$	Geometric Neutral Point of Wing
Re	Reynolds Number

r	Circle Radius in Circling
S	Wing Area
S_H	Horizontal Tail Area
V_{CAS}	Calibrated Air Speed
V_K	Circling Speed
x_H	Horizontal Tail Arm Referenced to Geometric Neutral Point of Wing
x_h	Horizontal Tail Arm Referenced to Center of Gravity
x_{N25}	Distance of Geometric Neutral Point from Leading Edge of M.A.C.
x_s	Distance of C.G. from Leading Edge of M.A.C.
α	Wing Angle-of-Attack
α_H	Horizontal Tail Angle-of-Attack
α_{HK}	Horizontal Tail Angle-of-Attack in Circling
α_0	Zero-lift Angle-of-Attack
$\Delta\alpha_H$	Incremental Horizontal Tail Angle-of-Attack
$\Delta\alpha_{HK}$	Incremental Horizontal Tail Angle-of-Attack due to Circling
η	Elevator Angle
Λ	Wing Aspect Ratio
Λ_H	Horizontal Tail Aspect Ratio
$\rho = 1.226\ kg/m^3$	Air Density
φ	Bank Angle in Circling
ω	Rotational Speed
ω_y	Rotational Speed Around y-Axis

WING

Span:	$b = 15\ m$
Area:	$S = 11\ m^2$
Aspect ratio:	$\Lambda = 20.45$
Mean aerodynamic chord:	$l_\mu = 0.75\ m$
Lift slope:	$dc_A/d\alpha = 5.73$
Zero-lift moment coefficient:	$c_{M25} = -0.1$
Zero-lift angle-of-attack:	$\alpha_0 = -3.8^0$

HORIZONTAL TAIL

Span:	$b_H = 2.5\ m$
Area:	$S_H = 1.1\ m^2$
Aspect ratio	$\Lambda_H = 5.68$
Lift slope:	$dc_{AH}/d\alpha = 4.45$
Horizontal tail area	$x_H = 3.82$
Elevator deflections:	$\eta = 18^0$ bis -22^0

INTRODUCTION

After the V-tail and the all-moving tail, the fixed horizontal stabilizer (plus elevator) has been rediscovered. Despite a slight performance loss compared to the all-moving tail, the fixed horizontal tail shows an advantage because of a favorable effect on the handling characteristics of a sailplane. However, this generally accepted advantage should not cover up the fact that the operating range of the fixed horizontal tail is rather limited in terms of flight performance and characteristics. The limits of satisfactory flight characteristics in circling were obviously exceeded on a modified ASW-19.

After a wing section modification, it was expected that, instead of the previous thermalling lift coefficient of $c_L = 1.2$, $c_L = 1.4$ could be flown. However, the first thermalling flight showed that from a 30° bank on, a pitch oscillation occurred that was extremely difficult to compensate. At a 45° bank it was no longer possible to even maintain the speed corresponding to $c_L = 1.4$. The hoped for advantage of the wing modification appeared impossible to realise in thermalling. Only an aft movement of the C.G. provided the required improvement of the circling characteristics. The success of this measure is astonishing at first, as this should normally degrade the longitudinal stability and thus worsen the flight characteristics. In order to explain this effect of the C.G. shift, tail aerodynamics and flight mechanics in circling have to be investigated more throughly.

LIFT COEFFICIENT OF THE HORIZONTAL TAIL IN STRAIGHT FLIGHT FOR FORWARD AND AFT C.G. POSITIONS

For the following investigation of the tail aerodynamics and flight mechanics, the values of the ASW-19 (Table 1) are used. Fig. 1 shows the tail lift coefficient c_{L_H} in straight flight vs. speed for forward and aft C.G. locations (Ref. 1). The corresponding wing lift coefficients are plotted in steps of 0.2. At aft C.G. locations the tail creates down loads at high speed and lift at low speed. However, if the C.G. location is at the wing neutral point $x_{CG}/\bar{c} = .25$, which corresponds to the forward C.G. limit of the ASW-19, then the tail lift coefficient stays constant from high speed to low speed. The equation

$$c_{L_H} = \frac{S\,\bar{c}}{S_H\,\ell_H}\left[c_{L_W}\,\frac{x_{CG} - x_{N25}}{\bar{c}} + c_{M25}\right]$$

indicates this very clearly. As the thermalling is done mostly at the highest possible lift coefficients, the following investigations are done for a wing lift coefficient of $c_{L_W} = 1.4$ and the geometric data given in Fig. 1.

ANGLE OF ATTACK CHANGES FOR HORIZONTAL TAIL AS FUNCTION OF WING LOADING, LIFT COEFFICIENT AND BANK

The slightly changed wing load distribution in circling flight will not be dealt with here and shouldn't cause any problems for sailplanes with wing spans up to 15 m. The effect of circling on horizontal tail aerodynamics, however, cannot be ignored, especially for sailplanes that are often flown at large bank angles and small circle radii when thermalling. In Fig. 2 the mechanics of circling flight are depicted (ref. 2). For an airplane flying with the circling speed V_C on a circle with radius r, the rotational speed is

$$\Omega = V_C/r$$

As precise circling requires the bank angle φ, the airplane experiences a constant positive rotation around its y-axis. This rotational speed amounts to

$$\omega_y = \Omega \sin\varphi$$

The circling speed follows from ref. 3

$$V_C = \sqrt{\frac{W}{S}\frac{2}{\rho}\frac{g}{c}} \cdot \sqrt{\frac{1}{\cos\varphi}}$$

and the circling radius from

$$r = \frac{V_C^2}{g \cdot \tan\varphi}$$

The equation for the circling speed shows clearly that, at a constant bank and circling speed, the wing loading W/S and c_L are linearly inter-dependent, i.e., a 20% increase in c_L corresponds to a 20% decrease in wing loading. This relationship should be kept in mind for the following evaluations.

The rotational speed Wy around the C.G. also influences the angle-of-attack of the horizontal tail. As shown in Fig. 3, the tail angle-of-attack α_H is increased by $\Delta\alpha_{HC}$, the tail angle-of-attack increment due to circling. This angle $\Delta\alpha_{HC}$ is dependent on the tail arm ℓ_h, the rotational speed ω_y and the circling speed V_C

$$\Delta\alpha_{HC} = \text{arctg} \frac{\ell_h \cdot \omega_y}{V_C}$$

In most cases this angle $\Delta\alpha_{HC}$ is smaller than 10° and a calculation in radius is sufficient:

$$\Delta\alpha_{HC} = \frac{\ell_h \cdot \omega_y}{V_C}$$

In Fig. 4 the incremental tail angle-of-attack $\Delta\alpha_{HC}$ is plotted for a wing lift coefficient $c_{L_W} = 1.4$ and for a wing loading

$W/S = 32\ kg/m^2$

against the circling radius r. Additionally, the circling speed V_C and the corresponding bank angle φ are given. For bank angles of $\varphi = 45°$ and $60°$, the results for a wing loading of

$W/S = 28\ kg/m^2$

are also shown. To compliment this, the same calculations are repeated for a lift coefficient $c_{L_W} = 1.2$ in Fig. 5.

For further investigations the values are restricted to a wing lift coefficient $c_{L_W} = 1.4$ and bank angles of $\varphi = 0$, 45 and 60 degrees. The effect of the tail boom, which has a damping effect just as the horizontal tail, and which can increase the incremental tail angle-of-attack $\Delta\alpha_{HC}$, according to Ref. 2, by 5 to 10%, is not taken into account.

THE EFFECT OF TAIL ANGLE-OF-ATTACK CHANGE ON FLIGHT HANDLING AND PERFORMANCE OF A SAILPLANE DUE TO CIRCLING

Figures 3, 4, and 5 indicate how the tail angle-of-attack increment due to circling increases with larger bank angles. On the other hand, the tail lift coefficient c_{L_H} required for steady-state circling is independent of the bank angle φ. An increase in tail lift coefficient due to circling has to be prevented by increasing upward elevator deflection. The amount of the elevator deflection can be established from the section lift curves with the elevator angle η as parameter (Ref. 4). Fig. 6 also shows the section polar c_ℓ vs. c_d which indicates the substantial drag increase when leaving the laminar bucket. For the following investigation the extent of the laminar bucket is indicated by a dashed line in the c_ℓ vs. α curves. Fig. 7 shows, somewhat enlarged, the area of further interest from Fig. 6.

To facilitate the analysis of this diagram, the lift curves c_ℓ vs. α for the required negative elevator angles are plotted too. The lift coefficients of the horizontal tail for the wing lift coefficient $c_{L_W} = 1.4$ are taken from Fig. 1 and amount to $c_{L_H} = .35$ for the forward C.G. location and $c_{L_H} = -.20$ for the forward C.G. location.

The tail angle-of-attack for straight flight at $\varphi = 0$ degrees. can be calculated as

$$\alpha_H = \frac{c_{L_H}}{dc_L/d\alpha} \cdot \left[1 - \frac{d\alpha_w}{d\alpha} \right] + \alpha_o + \varepsilon_H - \varepsilon_o$$

In this equation $dc_L/d\alpha$ denotes the lift slope, $1 - \frac{d\alpha_w}{d\alpha}$ the tail effectiveness or the downwash effect of the wing on the tail angle-of-attack, α_o the zero-lift angle of the wing, ε_H the horizontal tail incidence and ε_o

the wing incidence. For the ASW-19 the following values are used:

$$dc_L/d\alpha = 5.73$$

$$1 - \frac{d\alpha_w}{d\alpha} = 0.79 \text{ for } c_{L_W} = 1.4$$

$$\alpha_o = -3.8^\circ$$

$$\varepsilon_H = 3^\circ$$

$$\varepsilon_o = 5.25^\circ$$

Apart from the incidence angles ε_H and ε_o these values are difficult to determine. Addition of errors in one direction can reach 1°. The incremental tail angle-of-attack $\Delta\alpha_{HC}$ due to circling is determined according to Fig. 4, amounting to

φ	$\Delta\alpha_{HC}$
0°	0°
45°	2.8°
60°	4.2°

As the C.G. position has only little effect, it is ignored here.

The actual tail angle-of-attack as a function of bank angle at constant wing lift coefficient is then

$$\alpha_{HC} = \alpha_H + \Delta\alpha_{HC}$$

The resulting values c_{L_H} and α_{HC}

yield the points in Fig. 7 for the forward and aft C.G. positions. While the horizontal tail benefits in straight flight ($\varphi = 0^\circ$) almost over the entire C.G. range from the low drag in the laminar bucket, it operates from bank angles of 45° on the outside of the laminar bucket. This drag increase alone does not decrease the climb performance appreciably. It is more important that, at forward C.G. positions and bank angles of more than 45°, the elevator deflections due to tail angle-of-attack changes become increasingly non-linear.

In terms of flying this means that the pilot has to pull more elevator than at lower bank angles to compensate for a given tail angle-of-attack change. This leads to under or over-controlling by the pilot in relatively turbulent thermals, depending whether he is starting from a larger elevator angle to a smaller or vice versa. Even though the wing flow is still fully attached, the airplane begins to oscillate in pitch. The speed varies by 5 to 10 km/h accordingly. However, the pilot has to "feel" his way in the thermal and this requires constant speed which he can only regain at a wing lift coefficient clearly lower than $c_{L_W} = 1.4$, (example: at $c_{L_W} = 1.2$.).

This in turn requires a higher circling speed and a larger circling radius at a given bank angle. The better climb performance towards the center of the thermals cannot be realized, because the airplane cannot be flown at $c_{L_W} = 1.4$.

Fig. 8 explains this situation for the forward and aft C.G. positions. These curves are derived from cross-plotting Fig. 7 for $c_\ell = .35$ and $c_\ell = .25$. At the forward C.G. of $x_{CG}/\bar{c} = .25$, pitch control difficulties as described above can occur from bank angles of 30 deg. on. At 45° bank angle the maximum elevator deflection is reached. From this bank angle on it is no longer possible to stall the airplane in steady flight.

Fig. 9 shows the same curves again referenced to the same zero point. This indicates clearly the difference in elevator effectiveness between camber changes in the direction of lift or against it. For camber changes due to upward deflections with tail down loads, the decrease in elevator effectiveness occurs at somewhat higher elevator deflections than for tail lift.

Whether the above explained flight handling degradation is caused solely by elevator deflections of over ± 12° is not certain. Additionally, the fast forward movement of the transition point in the boundary region of the laminar bucket could have a noticeable influence on the elevator effectiveness. To what extent can only be determined from further aerodynamic investigations. To exclude any negative effects of the horizontal tail on the flight handling, the operating range of the horizontal tail should lie within the laminar bucket.

CONCLUSION

The degradation of handling characteristics explained above as originating from the horizontal tail cannot be ignored. They clearly influence the climb performance of sailplanes. Climb and penetration performances have, especially for 15 m sailplanes and for weather situations typical for Europe, about the same importance. This suggests evaluations on how to increase the operating range of the horizontal tail without performance losses.

After weighing all advantages and disadantages of different tail configurations, the all-moving tail with geared tab and the variable- incidence tail with elevator appear most suitable. The latter configurations combines the advantages of the all-moving tail and of the elevator on a fixed tail. By changing the tail incidence, the tail angle-of-attack can be adjusted to the optimum at all operating conditions. For Fig. 7 this would mean that a change in tail incidence by -4^{o} would be sufficient for both C.G. positions. The larger construction effort is disadvantageous but would be justified by the performance gains in thermalling. These considerations are especially applicable if either the wing lift coefficient is considerably increased or the wing loading significantly reduced.

SUMMARY

After the V-tail and the all-moving tail, the fixed tail is increasingly used again. It appears to represent the best compromise regarding flight performance and handling characteristics. Unfortunately, the laminar operating range is rather small. Especially in circling flight the limits of the optimum operating range are reached and sometimes exceeded.

In circling flight the airplane experiences a steady positive rotation around the y axis which increases the angle-of-attack of the horizontal tail. This incremental tail angle-of-attack has to be compensated by an upward elevator deflection to keep a constant tail lift coefficient. As long as the required elevator deflection increases linearly with the incremental tail angle and that has to be compensated, flight handling is not affected. However, this linear relation extends only to about 12^{o} elevator angle. For larger elevator angles the elevator change per incremental tail angle-of-attack increases so rapidly that steady circling becomes impossible. Because of this over-controlling tendency, disturbances caused by turbulence or by the pilot create a pitch oscillation. In this circling condition it is no longer possible to keep the speed even approximately corresponding to the maximum lift coefficient.

The effect described above was demonstrated on a modified ASW-19 (which can reach a maximum lift coefficient of 1.46) at a lift coefficient of 1.4. Degraded handling characteristics in circling flight reduce the climb performance; this affects the cross-country speed considerably, especially for the useable weather conditions in Europe.

After considering all advantages and disadvantages of various tail configurations, the all-moving stabilizer with geared tab and the variable-incidence tail with elevator appear best suited to improve handling characteristics and thus flight performance.

REFERENCES

[1] Schmaljohann, B., Einfluß der Leitwerksauslegung auf den Widerstand und Leitwerkswirksamkeit von Segelflugzeugen (Diplomarbeit).

[2] Morelli, P., Static Stability and

Control of Sailplanes.
[3] Thomas, F. Grundlagen für den Entwurf von Segelflugzeugen.
[4] Althaus, D., Stuttgarter Profilkatalog I. Meßergebnisse aus dem Laminarwindkanal des Instituts für Aerodynamik und Gasdynamik der Universitat Stutgart 1962-1972.

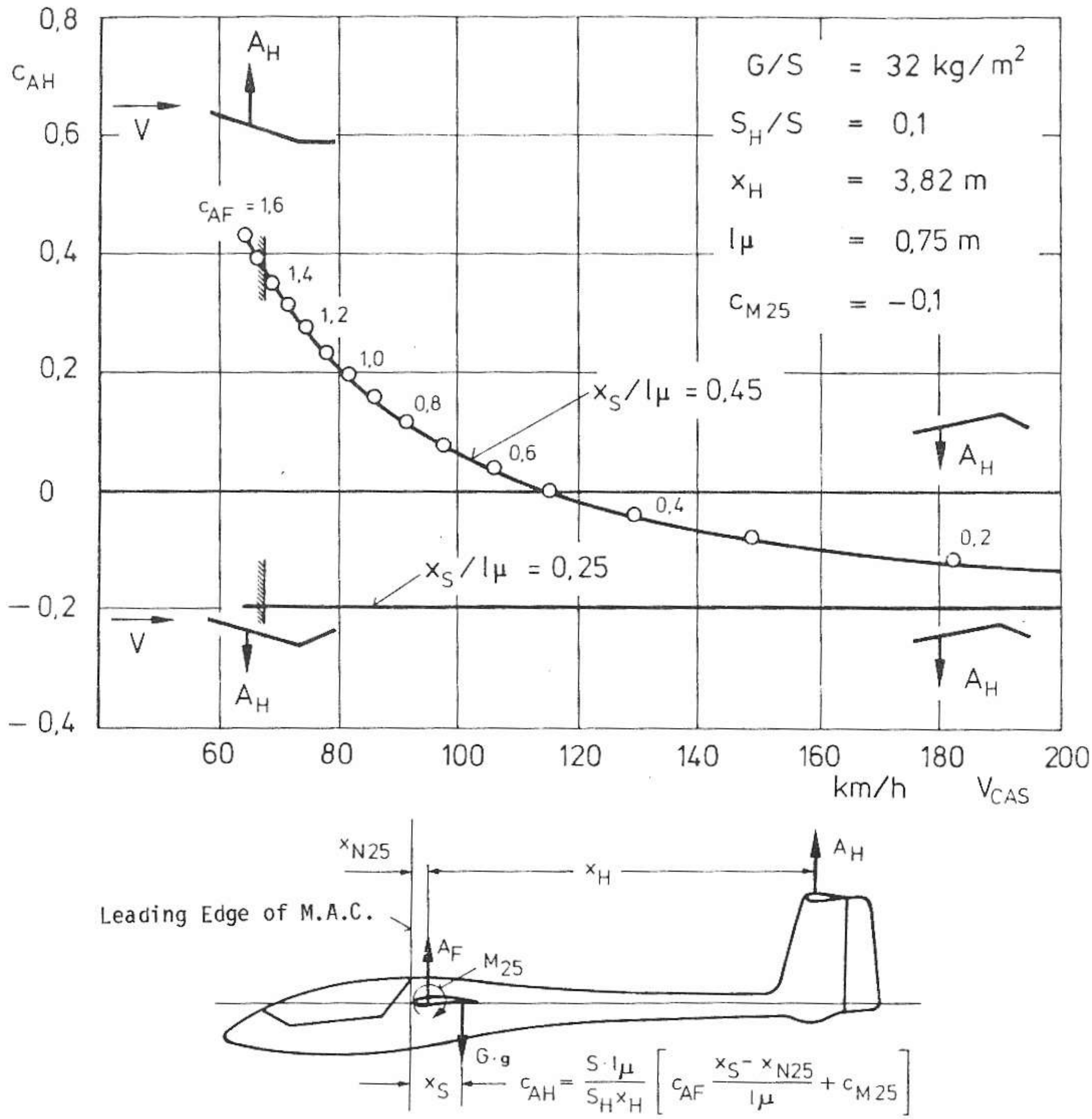

Fig. 1: Horizontal Tail Lift Coefficient for Forward and Aft C.G. Locations vs. Speed

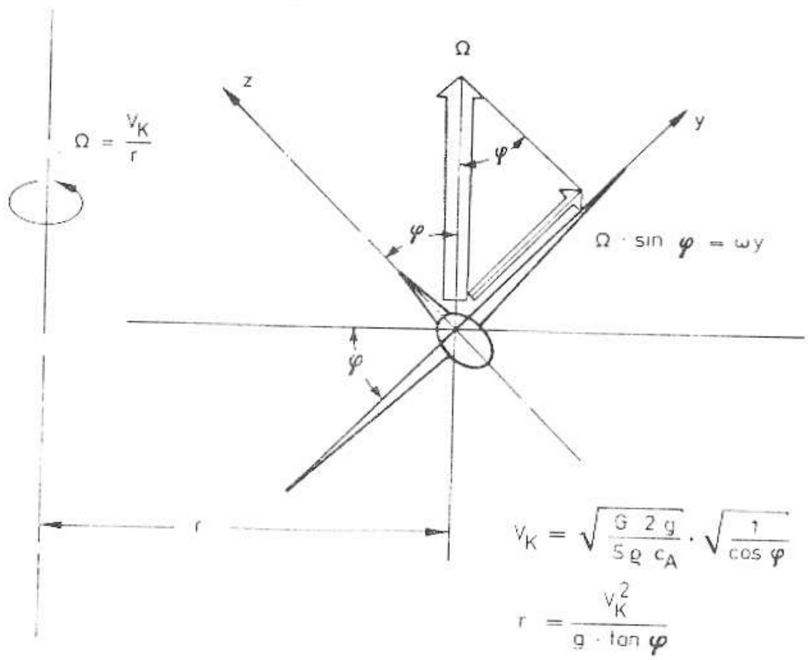

Fig. 2: Steady-State Rotational Speed around y-Axis in Circling

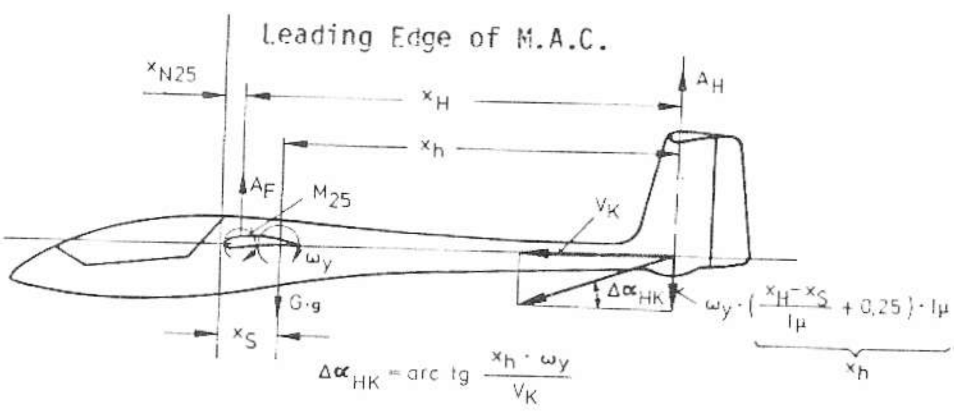

Fig. 3: Angle-of-Attack Increase at Horizontal Tail in Circling

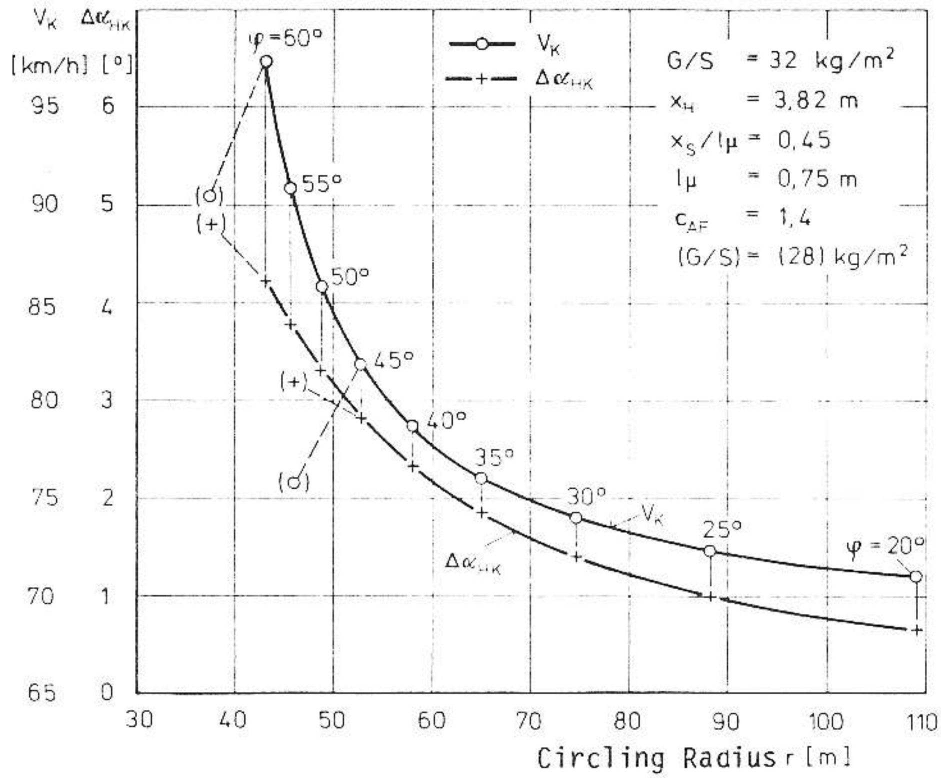

Fig. 4: Circling Speed and Incremental Horizontal Tail Angle-of-Attack vs. Circling Radius at c_{AF} = 1.4

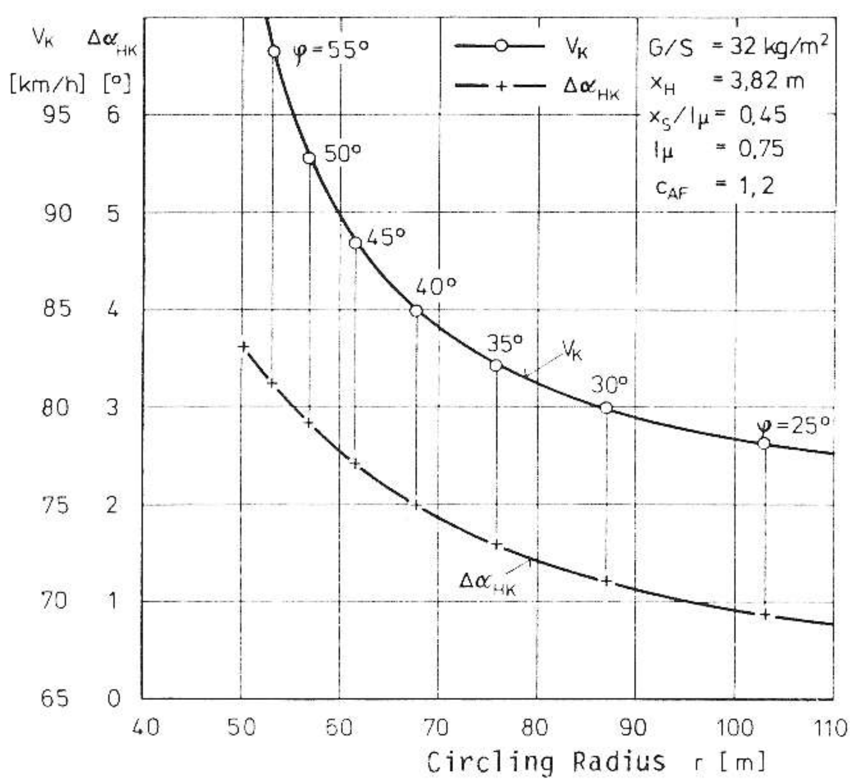

Fig. 5: Circling Speed and Incremental Horizontal Tail Angle-of-Attack vs. Circling Radius at c_{AF} = 1.2

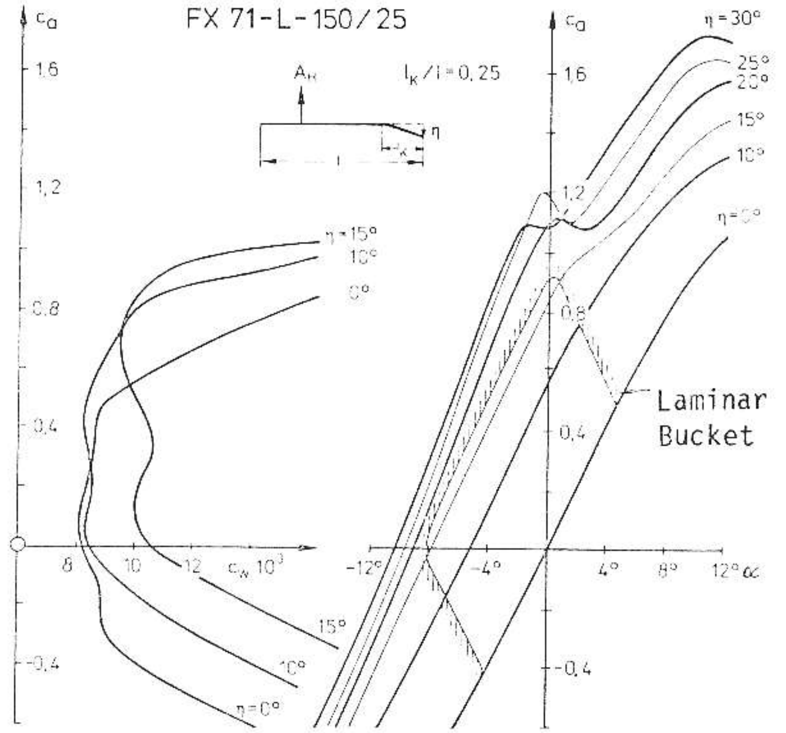

Fig. 6: Horizontal Tail Section FX 71-L-150/25

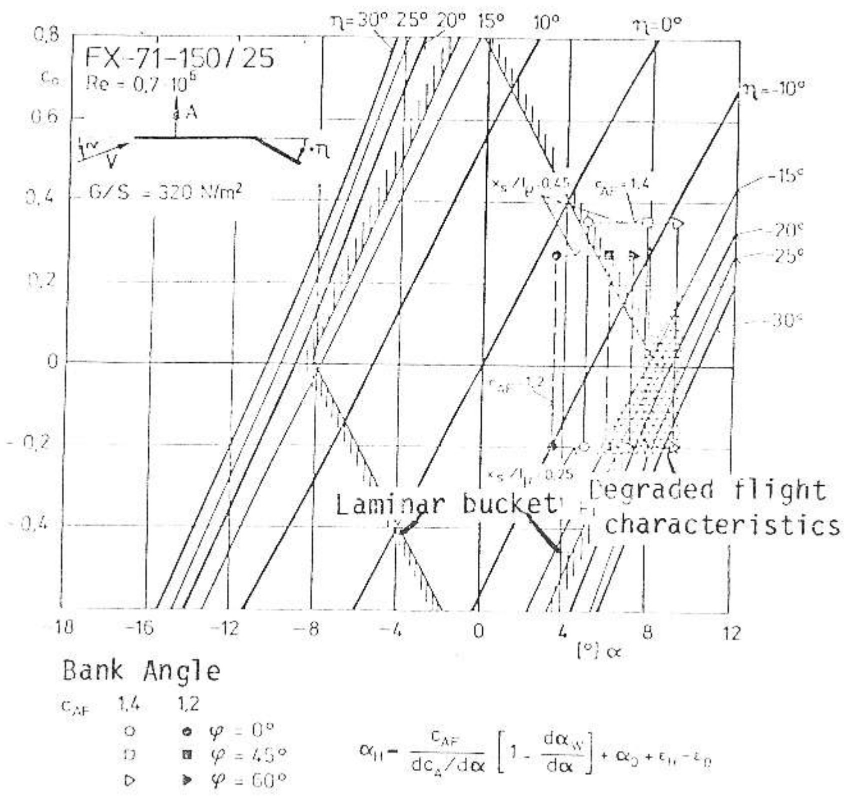

Fig. 7: Effect of Bank and C.G. Position on the Horizontal Tail Aerodynamics of the ASW-19

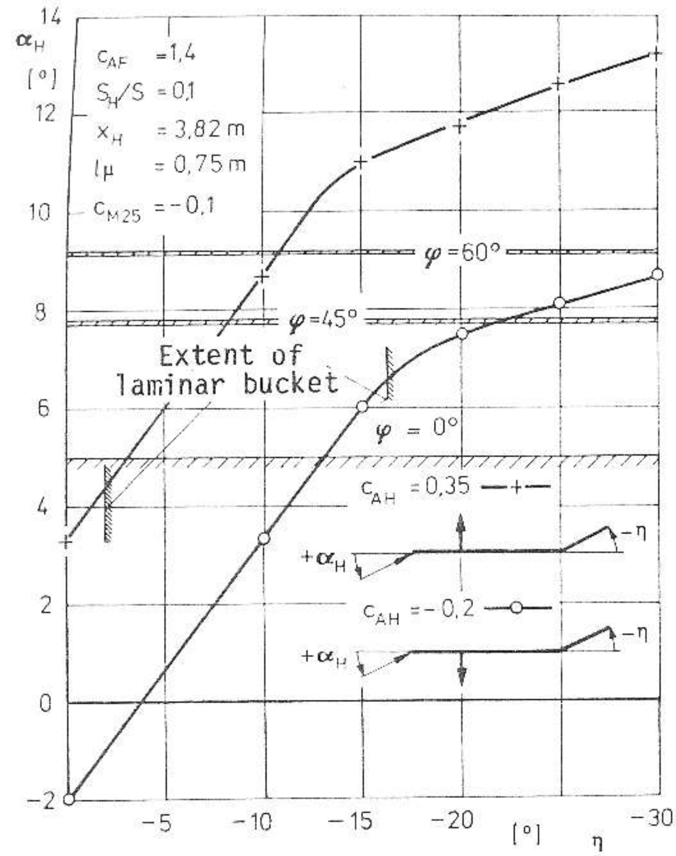

$x_S/l\mu = 0{,}45$ —+—

$x_S/l\mu = 0{,}25$ —o—

Fig. 8: Horizontal Tail Angle-of-Attack vs. Elevator Angle

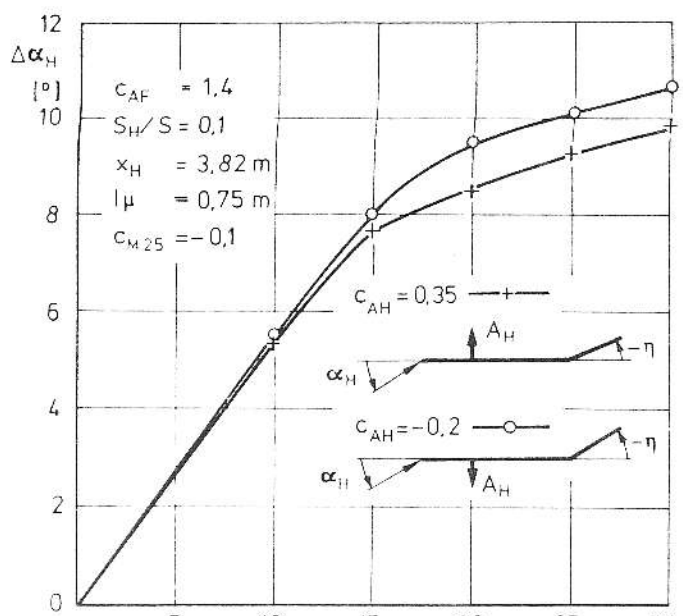

$x_S/l\mu = 0{,}45$ —+—

$x_S/l\mu = 0{,}25$ —o—

$\Delta\alpha_H = \alpha_H - \alpha_H(\eta = 0)$

Fig. 9: Change in Horizontal Tail Angle-of-Attack vs. Elevator Angle